María L. Ferreira, Saad A. Al-Bogami and Hugo I. de Lasa*

Self Diffusivity of n-Dodecane and Benzothiophene in ZSM-5 Zeolites. Its Significance for a New Catalytic Light Diesel Desulfurization Process

DOI 10.1515/ijcre-2015-0129

Abstract: This study provides theoretical support to a recent promising ZSM5 catalyst used for the selective desulfurization of light diesel type compounds (Al-Bogami and de Lasa 2013; Al-Bogami, Moreira, and de Lasa 2013). With this end, Molecular Dynamics (MD) simulations employing a rigid silicalite structure are developed to calculate self-diffusivities of n-Dodecane (n-C12) and Benzothiophene (BZT) in a silicalite structure. The simulations are performed at 573 K, 623 K, 673 K and 723 K at a fixed loading of 1 molecule per unit cell to study the temperature effect on diffusivity coefficient. In addition, a number of simulations which are developed to investigate four molecule loadings (corresponding to 0.25, 0.5, 0.75 and 1 molecule per zeolite unit cell) at 723 K. MD simulations, show a self diffusivity of BZT one order of magnitude higher than that of n-C12 self diffusivity at all temperatures investigated. This is the case in spite of BZT having a critical molecular diameter of 6 Å when compared to the 4.9 Å diameter of n-C12. In addition, the self diffusivity coefficient is found to increase with temperature for both n-C12 and BZT. Furthermore, the results obtained show that the self diffusivity of n-C12 decreases as the number of n-C12 molecules per zeolite unit cell increases. On the other hand, it is observed that the self-diffusivity coefficient for BZT remains fairly constant and drops at a loading of 1 molecule per zeolite unit cell only. These coefficients show that differences in n-C12 and benzothiophene diffusivities favours desulfurization with selective benzothiophene adsorption and sulfur species removal as coke (Al-Bogami and de Lasa 2013).

***Corresponding author: Hugo I. de Lasa,** Faculty of Engineering, Chemical Reactor Engineering Centre (CREC), Western University, London, Ontario, Canada N6A 5B9, E-mail: hdelasa@eng.uwo.ca
María L. Ferreira, PLAPIQUI-UNS-CONICET, Camino La Carrindanga Km 7 CC 7171, 8000 Bahía Blanca, R. Argentina
Saad A. Al-Bogami, Research and Development Centre, Saudi Aramco Oil Company, Dhahran, Saudi Arabia

Keywords: diesel, desulfurization, zeolite, catalyst, molecular simulation, self diffusion

1 Introduction

Zeolites are high crystalline aluminosilicate materials with a microporous structure formed of alumina [AlO_4^-] and silica [SiO_4] tetrahedra. They can be found naturally or as-synthesized and both have a wide range of applications (Hagen 2006). Zeolite properties especially acidity and shape selectivity make zeolites viable for many industrial applications. As catalysts, zeolites have shown to be an essential element for the oil refining industry since their first use in the sixties. For example, Fluid Catalytic Cracking (FCC) catalysts account for more than 95% of the world consumption of Y-type zeolites (Bogdanov et al. 2009; Marcilly 2001). The MFI-type zeolite especially the ZSM-5 is the second most used catalyst with main applications in catalytic cracking, alkylation of aromatics, xylene isomerization and catalytic dewaxing (Bogdanov et al. 2009). Recent research using H-ZSM5 as a desulfurization catalyst for FCC gasoline under mild conditions of pressure and temperatures showed promising results regarding the shape selectivity of H-ZSM5 towards sulfur species conversion (de Lasa, Hernandez-Enriquez, and Tonetto 2006; Jaimes, Ferreira, and de Lasa 2009, Jaimes, Badillo, and de Lasa 2011; Yu, Waku, and Iglesia 2003).

ZSM-5 zeolites are the aluminum-containing members of the MFI family, while silicalites are the members composed entirely of SiO_4 tetrahedra. In other words, silicalite is a pure silica zeolite with a system of straight channels interconnected by zigzag channels. The ZSM-5 structure is similar, however, with aluminum substituting for a small fraction of the silicon in the crystal lattice (Jia and Murad 2005; Liu et al. 2004). In general, ZSM-5 and silicalite are classified as high silica zeolites with a silica to alumina ratio typically above 10. ZSM-5 with a Si/Al ratio above 500 is sometimes referred to as silicalite (Auerbach, Carrado, and Dutta 2003; Govind et al. 2002;

Xiao 1990). The structure of a ZSM-5 zeolite has a 10-membered oxygen ring and two types of channel systems with a similar size: straight channels of 5.3 × 5.6 Å cross-linked with sinusoidal channels of 5.1 × 5.5 Å. These two different channels are perpendicular to each other and generate intersections with diameters of 9 Å. The ZSM-5 unit cell contains 96 T (Si or Al) atoms and 192 oxygen atoms with lattice constants of: a = 20.1 Å, b = 19.9 Å, and c = 13.4 Å (Govind et al. 2002; Liu et al. 2004; Xiao 1990; Zheng 2002). The pore structure of the silicalite is shown in Figure 1.

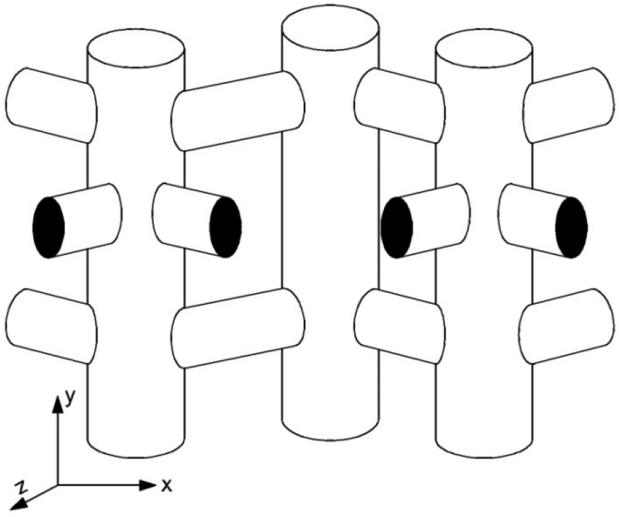

Figure 1: Schematic description of the silicalite pore structure (Adapted from Smit et al. 1997).

Heterogeneous catalytic processes necessarily proceed via at least the following five steps: (1) Diffusion of the reactants towards the catalyst surface, (2) Adsorption of the reactants on the catalyst active sites, (3) Chemical reaction at the active sites, (4) Desorption of the products from the active sites, and (5) Diffusion of the products away from the catalyst surface. In principle, any of the above mentioned five steps can be the rate determining step of the reaction. Therefore, it is crucial to understand the catalytic cycle process completely, considering the diffusion and adsorption steps. However, in zeolitic processes, the catalytic reaction takes place mainly inside the zeolite pores. Hence, it is important to characterize the diffusion of the reacting molecules in order to understand the phenomenon of shape selectivity (Lins and Nascimento 1997; Smit et al. 1997). Zeolite shape selectivity is the result of: (a) The difference in diffusivities of reactants and products; (b) The difference in the adsorption of reactants in zeolitic cavities of different sizes and shapes; (c) The transition state selectivity (Rozanska and Van Santen 2003).

The experimental techniques for measuring diffusion in zeolites can be classified into two main categories: macroscopic and microscopic methods. Macroscopic techniques typically use a bed of zeolite crystals or a zeolite membrane, and measure the response to a change of the adsorbate concentration in the surrounding gas phase. The interpretation of the response is mostly based on a description of the diffusion via Fick's law. As these experiments measure the response to a concentration change, these methods usually measure the transport diffusivity. Some macroscopic techniques are also used to measure self-diffusion by making use of labelled molecules. Macroscopic techniques include: (i) Uptake methods, (ii) Membrane permeation, and (iii) Chromatographic methods. Microscopic techniques, on the other hand, are capable of measuring the mobility of adsorbates in a much shorter time and length scale than the previous mentioned macroscopic techniques. Microscopic techniques can, in principle, measure the propagation of molecules through a single zeolite crystal, and can directly probe the underlying microscopic mechanisms of diffusion. Microscopic methods include: (i) Pulsed Field Gradient Nuclear Magnetic Resonance (PFG NMR), (ii) other NMR methods, (iii) Quasi-Elastic Neutron Scattering (QENS), and iv) Interference microscopy. In contrast, theoretical methods form a valuable addition to the available experimental techniques. These methods include: (i) Molecular Dynamics (MD) simulation, (ii) Monte Carlo simulation and (iii) Transition State (TST) method (Schuring 2002).

Since their first appearance, Molecular Dynamics simulations have become a standard tool in computational chemistry. MD simulations have been used extensively to study the diffusion of hydrocarbons in different zeolitic structures. They showed a better alternative for visualizing the diffusion process than other approaches, as they simulate the motion of the diffusing molecules inside the pores. In addition, they allowed assessing the self-diffusion coefficients in the host pores (Catlow et al. 1991; Szczygieł and Szyja 2005).

Diffusion in zeolites belongs to the configurational regime because the molecular diameter is comparable to the zeolite channel diameter. The configurational diffusion displays energies of activation much larger than Knudsen and molecular diffusion. This regime displays very small diffusivity coefficients, typically in the order of 10^{-10} to 10^{-12} cm^2 s^{-1}. In addition, there is a strong dependence of diffusivity coefficients on the size and shape of the diffusing molecules. Diffusivity of hydrocarbon molecules is increasing markedly with decreasing

molecular size (Al-Khattaf 2001; Satterfield 1980; Xiao et al. 1992a, 1992b; Zheng 2002).

Diffusion of short n-alkanes and alkenes (C1-C7) in silicalite and ZSM-5 was extensively studied using MD simulations by many authors (Catlow et al. 1991; Dumont and Bougeard 1995; Hernandez and Catlow 1995; Hussain and Titiloye 2005; Jianfen et al. 1999; June, Bell, and Theodorou 1992; Lins and Nascimento 1997; Nicholas et al. 1993).

However, only few studies considered long n-alkanes diffusion in silicalite. For example, n-dodecane (n-C12) self-diffusion in silicalite was studied by Runnebaum and Maginn (1997) using Molecular Dynamics simulation. Results showed an increase in self-diffusion coefficient with temperature. Jobic (2000) found the same temperature effect on n-dodecane diffusion in ZSM-5 zeolite using quasi-elastic neutron scattering (QENS). Self-diffusion coefficients obtained by QENS were two orders of magnitude smaller when compared to MD simulations. Table 1 compares the self-diffusion coefficients reported in the literature for n-dodecane obtained with both MD simulation and QENS. Jobic and Theodorou (2006) studied the self diffusivity of long n-alkanes (C8-C16) in silicalite and Na-ZSM5 using QENS at 300 K. It was found that the self-diffusion coefficient was always higher in silicalite than in Na-ZSM5. For example, n-dodecane self diffusivity was reported to be 5.3 times higher in silicalite than in Na-ZSM5. This observation was attributed to the presence of Na counter ions which are expected to slow down n-alkane diffusion in MFI zeolites. Diffusion of n-alkanes (C2-C14) in silicalite and Na-ZSM5 was investigated by Jobic et al. (2006) using PFG NMR and QENS. Both results were in a good agreement with the general trend, showing a decrease in self diffusivity as the chain length of n-alkanes increases. However, the diffusivities measured by PFG NMR were up to one order of magnitude lower than the diffusivities determined by QENS technique. This difference was explained as the result of internal diffusion barriers in MFI-type zeolites. Since PFG NMR typically monitors molecular displacement in a micrometer scale, the estimated diffusivities are affected by these transport resistance only. However, this is of no relevance for QENS where much shorter displacements are recorded. A comprehensive review considering n-alkanes diffusion in zeolites can be found in Jobic and Theodorou (2007).

Diffusion of aromatic hydrocarbons namely benzene, toluene, ethylbenzene, m-xylene, and o-xylene in H-ZSM5, H-Beta and H-MCM-22 was investigated experimentally using FTIR Spectrometry by Roque-Malherbe et al. (1995). The diffusivity coefficient was measured at different temperatures. In all cases, the diffusion coefficient was found to increase with temperature. Sastre et al. (1998) studied the self diffusivity of o- and p-xylene in a 10 and 12 member ring zeolite model using MD simulation. The study was performed employing a flexible zeolite framework at 500 K and 100 ps of simulation time. Different molecule loadings were investigated. In addition, FTIR spectrometry was used to measure the diffusion coefficient experimentally. Results showed that p-xylene diffuses faster than o-xylene in the two zeolites channels. The self diffusivity coefficient was higher in the case of low loading compared to high loading. However, diffusion coefficients obtained experimentally were three orders of magnitude lower than those found using MD simulations. The reason for this discrepancy can be found in the fact that the uptake methods like FTIR do not measure the self diffusivity, which is the quantity obtained using MD simulation.

Diffusion of C_7 hydrocarbons namely heptanes, 3-ethylpentane, methylcyclohexane, and toluene in microporous materials (y-Al_2O_3, Faujasite, and ZSM-5) was studied using MD by Szczygieł and Szyja (2005). Heptane was found to have the highest diffusivity in ZSM-5 while toluene has the lowest diffusion coefficient. These results were attributed to the flexibility of the heptane molecules as compared to the rigid ring structures of methylcyclohexane and toluene. Song, Sun, and Rees (2002) studied the diffusion and adsorption of cyclic hydrocarbons, namely benzene, p-xylene, cyclohexane and 1,4-dimethylcyclohexane in silicalite using the

Table 1: Self-diffusion coefficients of n-dodecane as reported in the technical literature.

Reference	Method	Temperature (K)	Diffusion coefficient
Runnebaum and	MD simulation	300	3.79
Maginn (1997)	Silicalite	350	3.82
$D_s \times 10^5$ (cm^2/s)		400	4.03
Jobic (2000)	QENS	300	1.6
$D_s \times 10^7$ (cm^2/s)	ZSM-5	350	3
		400	5

Monte Carlo simulation. This study considered a rigid zeolite framework at different temperatures. One important conclusion from these computations is that saturated hydrocarbons diffuse much more slowly than their aromatic equivalents. Using MD simulation, Rungsirisakun et al. (2006) studied benzene self-diffusion in siliceous ZSM5, FAU and MCM-22 zeolites. This study was performed at 300 K with different molecule loadings. It was found that the self-diffusion coefficient decreases as molecule loading increases. Table 2 reports a comparison between diffusion coefficient values found in different literature for some aromatic hydrocarbons.

The use of a fixed or flexible zeolite framework in MD studies is a controversial topic in the open literature. For example, Leroy, Rousseau, and Fuchs (2004) compared the self-diffusion coefficients for a series of n-alkanes in silicalite obtained by using rigid and flexible frameworks. This MD study showed that zeolite flexibility affects the adsorbate transport properties differently according to n-alkane length and loading. The self-diffusion was enhanced using a flexible silicalite for the lowest loading and the shortest alkanes namely methane and n-butane. However, this effect was not observed for long chain alkanes, namely n-hexane and n-octane. A detailed review about the flexibility of the framework in MD simulations of zeolites can be found in Demontis and Suffritti (2009).

Recent research by our group at CREC-UWO shows experimentally in a fluidized Riser Simulator that there is a significant difference in the conversion of hydrocarbon species in the diesel boiling point range when using a ZSM5 catalyst. One can notice that while benzothiophene is being selectively removed as coke, n-dodecane is converted very modestly (Al-Bogami and de Lasa 2013). These reactivity differences can be traced to the disparity between n-C12 and benzothiophene diffusivities favouring selective sulfur species adsorption. Clarification and further insights into this matter is of outmost importance for the establishment of riser/downer fluidized bed processes for reducing sulfur content in light diesel.

As a result, given the critical importance of this subject, the self diffusivity of light diesel fraction model hydrocarbons represented with n-dodecane and benzothiophene species, in a ZSM-5 zeolite is investigated using MD. The effect of temperature on the self-diffusion coefficient is studied at four different temperatures: 573 K, 623 K, 673 K, and 723 K. This temperature range is considered for a light diesel desulfurization process based on a ZSM-5 catalyst. In addition, the molecular loading effect on self diffusivity is explored using different loadings which correspond to 0.25, 0.5, 0.75, and 1 molecule per unit cell (u.c) of zeolite at 723 K.

2 Methodology

Molecular dynamics (MD) involves the stepwise integration of Newton's equations. If frictional forces are added to the equations of motion, Langevin dynamics becomes possible. Accelrys uses CASTEP (The Cambridge Serial Total Energy Package plane wave DFT) for Molecular Dynamics. MD in CASTEP is based on the velocity Verlet algorithm for integration of the equation of motion. The default time step can be as high as 1 fs with this algorithm because of its numerical stability and the conservation of the constant of motion. The efficiency of the method is due in large part to the introduction of wave function extrapolation between MD steps. In addition, charge density extrapolation is accounted for.

Several methods are available for controlling temperature and pressure. Depending on which state variables are kept constant (energy E, enthalpy H, number of particles N, pressure P, stress S, temperature T, and volume V), different statistical "ensembles" can be generated. A variety of structural, energetic, and dynamic properties can then be calculated from the averages or the fluctuations of these quantities over the ensemble generated. Both the isothermal ensemble (where heat is exchanged with a temperature bath to maintain a constant temperature) and the adiabatic ensemble (where no heat exchange

Table 2: Self diffusivity coefficients reported in the literature for aromatic hydrocarbons.

Reference	Method	Benzene	Toluene	O-xylene	p-xylene
Roque-Malherbe et al. (1995) $D_s \times 10^9$ (cm^2/s)	FTIR, H-ZSM5, 300 K	0.5	1	0.01	
Sastre et al. (1998) $D_s \times 10^6$ (cm^2/s)	MD simulation, ZSM-5, 500 K			7.79	25.18
Szczygieł and Szyja (2005) $D_s \times 10^6$ (cm^2/s)	MD simulation, ZSM-5		0.326		
Rungsirisakun et al. (2006) $D_s \times 10^6$ (cm^2/s)	MD simulation, 300 K	1.65			

occurs) can be considered as follows: a) constant temperature and pressure (NPT), b) constant energy and volume (NVE), c) constant pressure and enthalpy (NPH) and d) constant temperature and volume (NVT).

The constant-energy, constant-volume ensemble (NVE), also known as the "*microcanonical ensemble*" is obtained by solving the standard Newton equation without any temperature and pressure control. Energy is conserved when this (adiabatic) ensemble is generated. However, because of rounding and truncation errors during the integration process, there is always a fluctuation, or drift in energy. Nevertheless, to obtain suitable NVE data and to be able to construct the Mean Square Displacement (MSD) with time for selected compounds (which are required to obtain chemical species self- diffusion coefficients), two main conditions have to be met: a) The system should be at near the target temperature and b) The system should have quasi constant energy content.

Thus, to achieve this, improving NVE predictions, a good temperature control is required. One possible approach is to use the so-called "NVT-Nosé" thermostat (Nosé 1984). The NVT-Nosé involves a deterministic dynamics using a fictitious coordinate added to the Lagrangian of the system. The thermostat employs a feedback loop between the instantaneous kinetic energy and the required temperature. The rate of feedback is determined by the parameter, *Q*. This parameter is selected so that the natural oscillation frequency of the Nosé coordinate is close to the characteristic frequency of the actual system.

In the case of the present study the ZSM5 zeolite structure was represented by a siliceous MFI (silicalite) without Al substitution in the framework. A supercell containing eight (2 × 2 × 2) unit cells (2,304 atoms) superimposed along the c axis was constructed, with unit cell parameters a = 20.076 Å, b = 19.926 Å and c = 13.401 Å. This structure contains two interconnecting channel systems.

The straight channels run parallel to the b-axis (010) and present elliptical cross-sections with minor and major axes of 5.2 Å and 5.8 Å, respectively. The sinusoidal (zigzag) channels run along the a-axis (100) and present a more circular but still elliptical cross-section (5.1 Å–5.2 Å) slightly smaller than the one of the straight channels. The intersection between these channels has a diameter of 9 Å. Figure 2 shows the structure of the ZSM-5 supercell used throughout the current simulation work.

The interaction between the zeolite framework and the hydrocarbons was described by using a COMPASS (Condensed-Phase Optimized Molecular Potentials for Atomistic Simulation Studies) Force Field (Bunte and Sun 2000; McQuaid, Sun, and Rigby 2004; Sun, Ren, and Fried 1998). Before starting any Molecular Dynamic simulation, the zeolite structure and the hydrocarbon molecules were optimized and their energy minimized. Following this step, the n-dodecane or benzothiophene molecules were introduced inside the zeolite structure randomly. A load of 1 molecule per unit cell (8 molecules/supercell) was considered and the initial velocities were assigned according to a Maxwell-Boltzmann distribution corresponding to the required temperature.

The system was then thermalized for 25 ps (picosecond) using a canonical NVT ensemble, including a constant number of atoms, a constant system volume, and a constant system temperature. The NVT ensemble was coupled with a NHL (Nose-Hoover-Langevin) thermostat (Samoletov, Dettmann, and Chaplain 2007).

Using the data from NVT, Molecular Dynamics runs were then performed within a microcanonical NVE ensemble having a constant number of atoms, a constant system volume, and a constant system energy or equivalent to adiabatic conditions. This was done at different temperatures with a fixed zeolite structure. The equations of motion were then integrated under these conditions using the Verlet algorithm (Verlet 1967) with an integration time step of 1 fs (femtoseconds) which is small enough to ensure energy conservation.

As a result of the above described simulation procedure, one can define an average mean square displacement (MSD) for all moving particles. This was obtained from the coordinate data stored in the trajectory files as follows:

$$\mathrm{MSD} = (\Delta \mathrm{R}(\mathrm{t}))^2 = \sum\nolimits_{\mathrm{i}} \left\langle \mathrm{r_i}(0) - \mathrm{r_i}(\mathrm{t}) \right\rangle^2 \tag{1}$$

where r_i represents the coordinates of molecule i, t is the simulation time in picoseconds (ps) and the ensemble average is over all the molecules in the simulation.

Given the calculated MSD, a self-diffusion coefficient D_s, was then extracted using Einstein's relation as in (eq. (2))

$$\mathrm{D_s} = \frac{1}{6\mathrm{t}} \left\langle (\Delta \mathrm{R}(\mathrm{t}))^2 \right\rangle \tag{2}$$

Consequently, one can deduce that

$$\mathrm{D_s} = \frac{\mathrm{a}}{6} \tag{3}$$

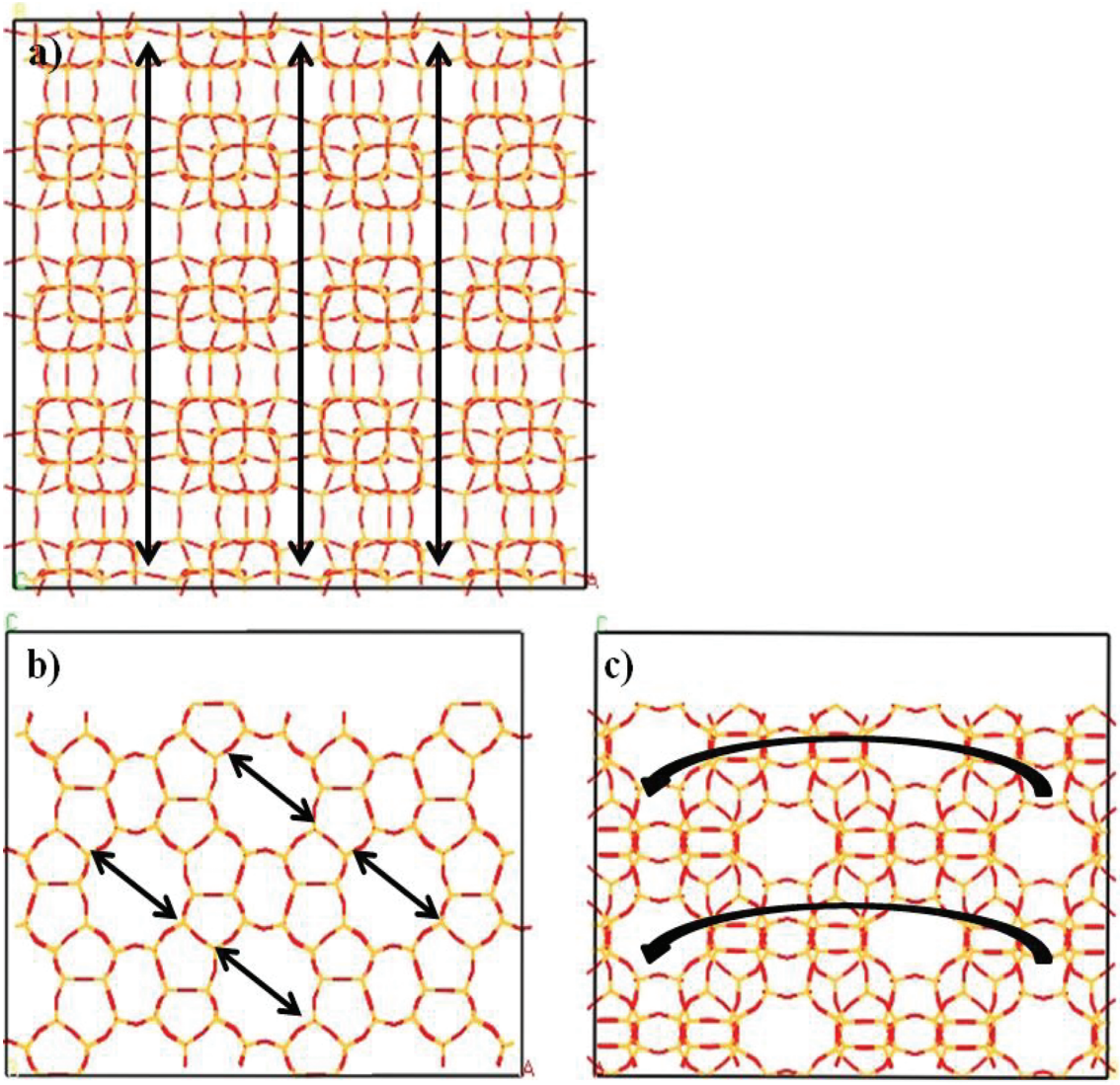

Figure 2: 2D views of a ZSM-5 supercell (8 unit cells) used in the current study with arrows indicating. (a) The straight channels location, (b) the intersections of straight and zigzag channels, and (c) the zigzag channels locations.

where a, is the slope of the linear least square fit of MSD versus simulation time.

Figure 3 reports a typical MSD curve. It is important to emphasize that when calculating the self-diffusion coefficient, the initial quadratic segment of the MSD curve is discarded. This is the case given that the initial sharp rise in the MSD plot is a result of a non-steady molecule behaviour while filling the available free volume. This non-diffusive motion continues until collisions with the channel walls or other molecules take place. After the movement in this initial phase, the MSD starts reflecting the actual translational diffusion of the adsorbate molecules (Lins and Nascimento 1997; Nicholas et al. 1993).

For example, in the case of n-C12 as reported in Figure 3, up for a total extended calculation time of 10,000 ps, one can see that the linear trend and as a result, the diffusivity coefficient remains unchanged. Thus, the nC12 diffusivity coefficient remains unaffected while the n-C12 is transported 7.74A which is in the range of the ZSM5 zeolite unit cell size.

Furthermore, for the purpose of calculation stability, different simulation times (50, 100, 200, 300, and 400 ps) were used with two temperatures (573 and 723 K). The results are discussed in the next section of this manuscript.

All MD simulation runs were carried out, visualized, and analyzed carefully using Forcite module of Accelrys Inc. Materials Studio 6.0 software installed on CMLP-3331

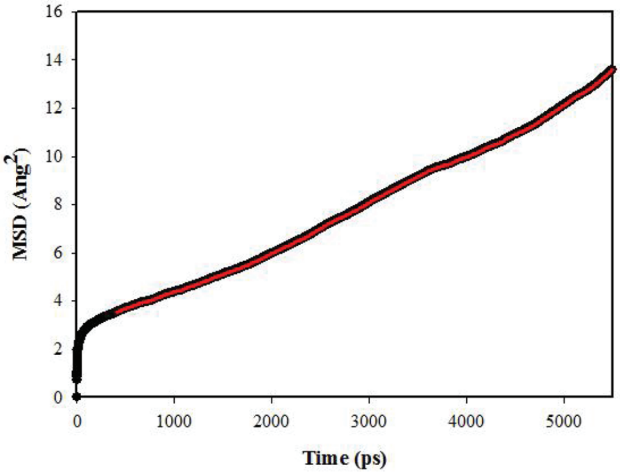

Figure 3: Mean square displacement (MSD) versus simulation time for the diffusion of 8 n-C12 molecules. Total simulation time was 5,500 ps with the full line representing the data between 400–5,500 ps with its R^2 regression coefficient being 0.9956.

computer station at the University of Western Ontario, Canada and Plapiqui-Conicet, Argentina.

3 Results and discussion

3.1 Self diffusivity calculations stability

As already stated, the stability of self diffusivity calculations for both n-dodecane and benzothiophene were investigated at 573 K and 723 K considering different simulation times (50, 100, 200, 300, and 400 ps) in the present study.

Figures 4 and 5 report the self-diffusion coefficient for n-C12 and BZT, respectively, as a function of the

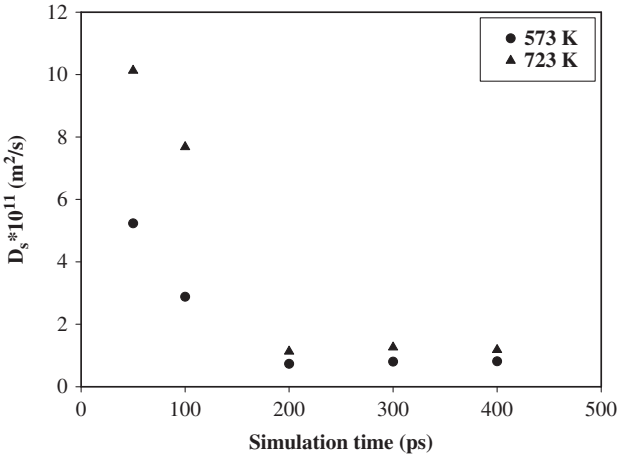

Figure 4: Self diffusivity of n-dodecane as a function of simulation time (molecule loading = 1/u.c).

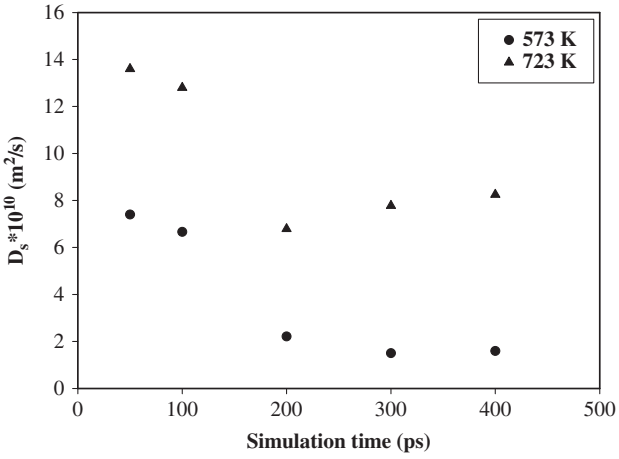

Figure 5: Self diffusivity of benzothiophene as a function of simulation time (molecule loading = 1/u.c).

simulation time and temperature. Results always show a higher self diffusivity at low simulation times (50 and 100 ps). Following this initial period, self diffusivity values obtained become both lower and stabilized at a simulation times of 300 and 400 ps. It should be mentioned that this generic behaviour was observed for both n-C12 and BZT cases.

On the basis of the results reported in Figures 4 and 5, it is considered that 400 ps is an adequate total molecular dynamic simulation time to establish self diffusivity coefficients as attempted in the present study

3.2 Self diffusivity of n-Dodecane

n-Dodecane is a normal paraffin with 12 carbon atoms and a 4.9 Å molecular diameter (Tukur and Alkhattaf 2005). Since the ZSM-5 zeolite exhibits dimensions of 5.2 × 5.8 Å and 5.1 × 5.2 Å for straight and zigzag channels respectively, n-dodecane is expected to have no diffusional constraints.

3.2.1 Temperature Effect on n-Dodecane Self Diffusivity

The self-diffusion coefficient of n-dodecane was found to increase noticeably with temperature. This result is shown in Figure 6 where the self diffusivity as a function of temperature is reported. For example, the self-diffusion coefficient of n-C12 at 723 K is about 1.5 times greater than that at 573 K. The same effect of temperature on n-C12 self diffusivity was found by Runnebaum and Maginn (1997) in silicalite structures using MD simulations. In addition,

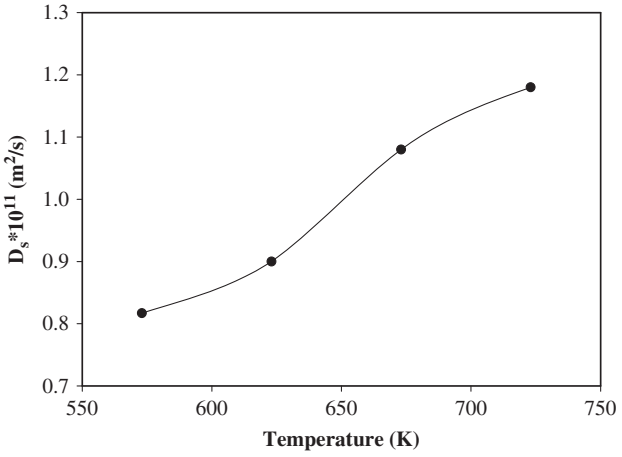

Figure 6: Self diffusivity of n-dodecane as a function of temperature (molecule loading = 1/u.c, and simulation time is 400 ps).

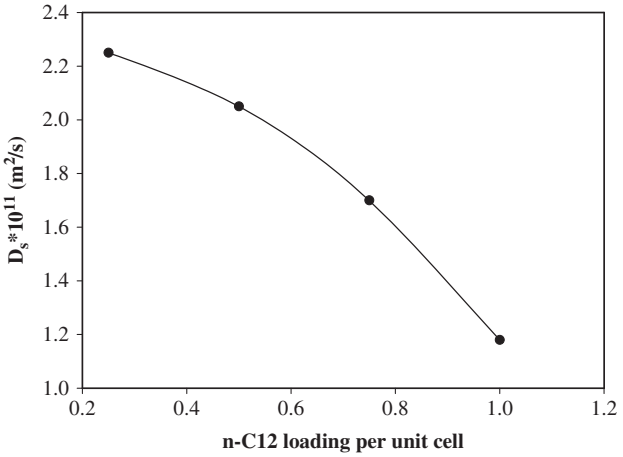

Figure 7: Self diffusivity of n-dodecane as a function of molecule loading per unit cell (Temperature is 723 K and simulation time is 400 ps).

using the experimental technique QENS, the same effect of temperature on the self diffusivity of n-dodecane was observed by Jobic (2000). Chain molecules, such as n-C12, can be thought of as becoming "flexible" as temperature is increased. However, with its inherent increased flexibility, the "chain like" molecule can move rapidly between structure configurations. This process continues until n-C12 adopts the configuration with the lowest barrier to diffusion. Thus, the self diffusivity coefficient is as a result increased (Runnebaum and Maginn 1997).

3.2.2 Molecule Loading Effect on n-Dodecane Self Diffusivity

The effect of change of molecule loading per unit cell (concentration) on self diffusivity coefficient for n-dodecane was studied at a constant temperature (723 K). Results obtained showed a concentration dependence of the self diffusivity as reported in Figure 7.

Kärger and Pfeifer (1987) described five different types of concentration dependencies of the self diffusivity (obtained with PFG NMR measurements). In general, these concentration dependencies were ascribed to differences in the interaction between the framework atoms and diffusing molecules. For example, interactions with different cations in the zeolites or the presence of strong and weak adsorption sites can result in these dependencies (Schuring 2002). On this basis, the observed behaviour of n-dodecane self-diffusion with the loading in this study belongs to Type I. This type of dependency was found for molecules adsorbed on large pore zeolites and undergoing no specific interaction (Kärger and Pfeifer 1987).

A similar effect of n-dodecane molecule loading per unit cell on self diffusivity is in general agreement with Nicholas et al. (1993) and Hussain and Titiloye (2005). These authors found however this behaviour for shorter n-alkane molecules (methane, ethane, and propane) in silicalite at 300 K and 400.

3.3 Self diffusivity of benzothiophene

Benzothiophene is a sulfur containing compound with a kinetic molecular diameter of 6 Å (Contreras et al. 2008) compared to 5.2 × 5.8 Å and 5.1 × 5.2 Å channels of the ZSM-5 zeolites. The upper critical molecular diameter required for chemical species to evolve in ZSM-5 zeolites is 6.6 Å (0.66 nm) or smaller which corresponds to durene (tetra-methyl-benzene). Durene is the molecule with the largest critical diameter able to diffuse out of the ZSM-5 zeolites during methanol conversion (Ravella, de Lasa, and Mahay 1987). Based on this fact, benzothiophene can still diffuse inside the ZSM-5 pores.

3.3.1 Temperature Effect on Benzothiophene Self Diffusivity

Figure 8 reports the self-diffusion coefficient of BZT at different temperatures (fixed loading of 1 molecule per zeolite unit cell and fixed simulation time of 400 ps). It can be observed that there is a BZT self diffusivity increase with temperature. The increase of BZT self diffusivity is very noticeable (about 5 times) as temperature changes from 573 K to 623 K, and becoming more modest afterwards.

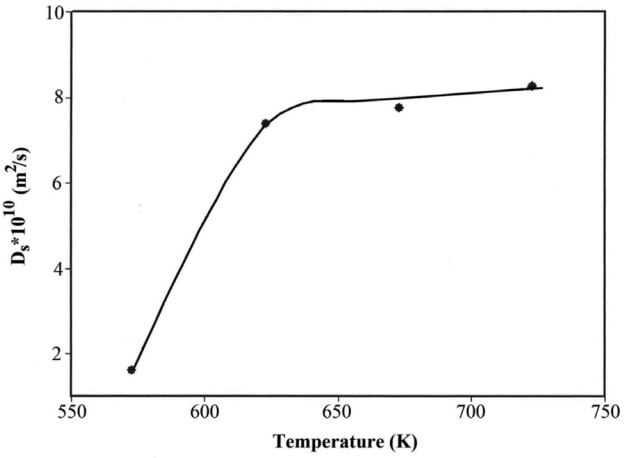

Figure 8: Self diffusivity of benzothiophene as a function of temperature (molecule loading per unit cell = 1/u.c, and simulation time is 400 ps).

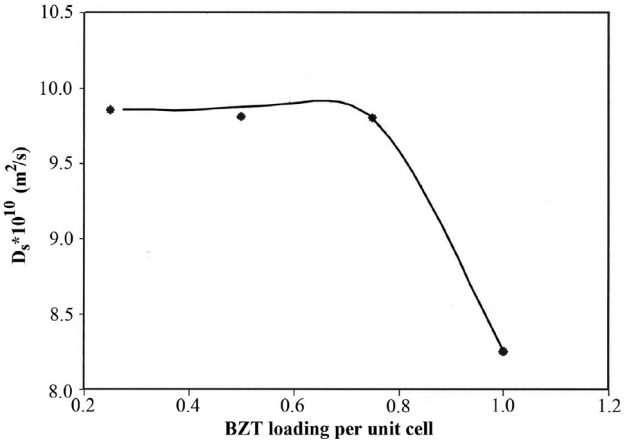

Figure 9: Self diffusivity of benzothiophene as a function of molecule loading per unit cell (Temperature is 723 K and simulation time is 400 ps).

Regarding this result, it is very important to highlight that diffusion studies of benzothiophene in ZSM-5 zeolites are absent in the technical literature. It is believed however, that reported diffusion studies of aromatic hydrocarbons can be considered for the purpose of comparing the obtained results. Sastre et al. (1998) reported the self diffusivity obtained using MD simulations for o- and p-xylene in a flexible model of 10 and 12 member ring zeolites. Self diffusivity values found were in the same order of magnitude (10^{-10} m^2/s) as BZT self diffusivity calculated in the current research. In addition, toluene self diffusivity in ZSM-5 produced a coefficient of the same order of magnitude as shown by Szczygieł and Szyja (2005) using MD simulations.

Concerning the benzothiophene self diffusivity calculated at various temperatures, they showed values of one order of magnitude higher than that for n-dodecane. This is in spite of the fact that benzothiophene has a kinetic molecular diameter of 6 Å while compared to 4.9 Å of n-dodecane. These results can be explained given the BZT molecule rigidity when compared to the long chain of n-dodecane molecule. The BZT molecule structure could be considered to move inside the ZSM-5 zeolite pores as a "free ball" while the n-dodecane molecule moves as a "spaghetti shaped" chain.

3.3.2 Molecule Loading Effect on Benzothiophene Self Diffusivity

The concentration dependence of self diffusivity on BZT was studied at different molecule loadings and 723 K. Results are reported in Figure 9. One can notice that BZT self diffusivity remains fairly constant and drops sharply at a loading of 1 molecule per unit cell. It is interesting to see that this behaviour resembles Type II of the five self diffusivity patterns reported by Kärger and Pfeifer (1987). The observed decrease in the self-diffusion coefficient at a sufficiently high concentration of BZT is an understandable consequence of mutual hindrance. This effect of mutual hindrance is found to be most significant for the large molecules (Kärger and Pfeifer 1987).

Sastre et al. (1998) found that self diffusivity of o-xylene, in a model structure of ZSM-5, is reduced with molecule loading increase. Another MD simulation study reported the same observation for benzene diffusion in the ZSM-5 zeolites (Rungsirisakun et al. 2006). It is speculated that such a decrease in self diffusivity is a result of steric hindrance "friction" between diffusing molecules passing each other.

In the current study, the significant decrease in benzothiophene self diffusivity at a molecule loading of 1 molecule/u.c can be attributed to the same issue. This friction between BZT molecules appears, however, not to be significant at low loadings (0.25, 0.5, and 0.75 molecules/u.c) as the self-diffusion coefficient remains fairly constant at these conditions.

4 Significance of the results obtained for the catalytic desulfurization of light diesel

Simulations in the present study were performed using a high level parametrization in the forcefield COMPASS.

COMPASS (Condensed-phase Optimized Molecular Potentials for Atomistic Simulation Studies) (Sun, Ren, and Fried 1998). This is a break-through in forcefield method. It is the first ab initio forcefield that enables accurate and simultaneous prediction of gas-phase properties (structural, conformational, vibrational, etc.) and condensed-phase properties (equation of state, cohesive energies, etc.) for a broad range of molecules and polymers. It is also the first high quality forcefield to consolidate parameters of organic and inorganic materials. (reference). The calculation was also developed with a careful checking of the control of the temperature, not easily achieved with other versions of Accelrys or even with other temperature parametrizations.

Results reported in this study provide evidence that there are significant differences in the benzothiophene and n-C12 self-diffusivities in ZSM5 zeolite. Self-diffusivity differences promote benzothiophene selective adsorption in the early stages of the unsteady reaction in the CREC Riser Simulator, as it can happen in a full industrial riser/downer circulating fluidized unit (de Lasa 1992).

In this manner, sulfur containing compounds have the increased opportunity of being removed as coke leaving the main species contributing to light diesel quality essentially unchanged (e.g. n-C12). It is important to emphasize that the conditions selected for the MD simulations include the 350–450°C range which is the expected temperature for the proposed new desulfurization process (Al-Bogami and de Lasa 2013).

5 Conclusions

(a) Molecular Dynamics simulation allows calculating self-diffusion coefficients for BZT and n-dodecane.
(b) Calculated self diffusivity coefficients show higher values for BZT than n-dodecane. This is true at all temperatures and in spite of BZT having a larger molecular diameter of 6 Å when compared to the 4.9 Å diameter of n-dodecane.
(c) Results obtained are consistent with the BZT molecule rigid configuration and this while compared to the "chain like" n-dodecane molecule. As a result, BZT molecules can move more freely than the n-dodecane molecules in ZSM-5 zeolites.
(d) Simulation results obtained are relevant for a desulfurization process to be implemented in a riser/downer fluidized unit where light diesel sulfur containing species can diffuse faster and as a consequence can be removed selectively using ZSM5 zeolites. This allows light diesel desulfurization with minimum paraffin cracking and hence, retaining the diesel quality.

Acknowledgments: The authors would like to acknowledge the financial contribution of the Natural Science and Engineering Research Council of Canada (NSERC). The authors also are very appreciative to Saudi Aramco Oil Company for providing the scholarship to Mr. Saad Al-Bogami and to the Consejo Nacional de Ciencia y Tecnologia (CONICET), for supporting Dr.M.L. Ferreira's research at Plapiqui, Univ.Nacional del Sur,Argentina. In addition, we would like to thank Ms. F. de Lasa for her assistance on the preparation of this manuscript.

Notation

BZT	Benzothiophene
C	concentration
COMPASS	Condensed-Phase Optimized Molecular Potentials for Atomistic Simulation Studies
CREC	Chemical Reactor Engineering Centre
D_s	Self diffusivity coefficient
FCC	Fluid Catalytic Cracking
FTIR	Fourier Transform Infrared Spectroscopy
MD	Molecular Dynamics
MFI	Mordenite Framework Inverted
MSD	Mean square displacement
PFG NMR	Pulsed Field Gradient Nuclear Magnetic Resonance
NVE	constant number of particles, volume, and energy
NVT	constant number of particles, volume, and temperature
NHL	Nose-Hoover-Langevin
n-C12	n-Dodecane
QENS	Quasi-Elastic Neutron Scattering
r	coordinate of a particle
Si/Al	silica to alumina ratio
t	simulation time
TST	Transition State
u.c	unit cell
ΔR(t)	change of particle coordinates with simulation time

Units

Å	Angstrom
°C	Celsius
cm^2	Squared centimetres
fs	Femtoseconds (10^{-15} s)
K	Kelvin
m^2	Squared metres
nm	nanometre
ps	Picoseconds (10^{-12} s)
s	seconds

References

1. Al-Bogami, S.A., de Lasa, H.I., 2013. Catalytic Conversion of Benzothiophene Over a H-ZSM5 Based Catalyst. Fuel 108, 490–501.
2. Al-Bogami, S.A., Moreira, J., de Lasa, H.I., 2013. Kinetic Modeling of Benzothiophene Catalytic Conversion Over a H-ZSM5 Based Catalyst. Ind. Eng. Chem. Res. 52, 17760–17772. DOI: 10.1021/ie401169k.
3. Al-Khattaf, S., 2001. Diffusion and Reaction of Hydrocarbons in FCC Catalysts. PhD thesis, University of Western Ontario.
4. Auerbach, S.M., Carrado, K.A., Dutta, P.K., 2003. Handbook of Zeolite Science and Techology, Marcel Dekker Inc, New York.
5. Bogdanov, B., Georgiev, D., Angelova, K., Hristov, Y., 2009. Synthetic Zeolites and Their Industrial and Environmental Applications, in: International Science Conference, Bulgaria.
6. Bunte, S.W., Sun, H., 2000. Molecular Modeling of Energetic Materials: The Parameterization and Validation of Nitrate Esters in the COMPASS Force Field. J. Phys. Chem. B 104, 2477–2489.
7. Catlow, C., Freeman, C.M., Vessal, B., Leslie, M., 1991. Molecular Dynamics Studies of Hydrocarbon Diffusion in Zeolites. J. Chem. Soc. Faraday Trans. 87, 1947–1950.
8. Contreras, R., Cuevas-Garcia, R., Ramirez, J., Ruiz-Azuara, L., Gutierrez-Alejandre, A., Puente-Lee, I., Castillo-Villalon, P., Salcedo-Luna, C., 2008. Transformation of Thiophene, Benzothiophene and Dibenzothiophene over Pt/HMFI, Pt/HMOR and Pt/HFAU: Effect of Reactant Molecular Dimensions and Zeolite Pore Diameter over Catalyst Activity. Catal. Today 130, 320–326.
9. de Lasa, H.I., 1992. Riser simulator U.S. Patent 5 102 628.
10. de Lasa, H.I., Hernandez-Enriquez, R., Tonetto, G., 2006. Catalytic Desulfurization of Gasoline via Dehydrosulfidation. Ind. Eng. Chem. Res. 45, 1291–1299.
11. Demontis, P., Suffritti, G.B., 2009. A Comment on the Flexibility of Framework in Molecular Dynamics Simulations of Zeolites. Microporous Mesoporous Mater. 125, 160–168.
12. Dumont, D., Bougeard, D., 1995. A molecular dynamics study of hydrocarbons adsorbed in silicalite. Zeolites 15, 650–655.
13. Govind, N., Andzelm, J., Reindel, K., Fitzgerald, G., 2002. Zeolite Catalyzed Hydrocarbon Formation from Methanol: Density Functional Simulations. Inter. J. Mol. Sci. 3, 423–434.
14. Hagen, J., 2006. Industrial Catalysis a Practical Approach, 2nd ed. Wiley-Vch, New York.
15. Hernandez, E., Catlow, C., 1995. Molecular Dynamics Simulations of n-Butane and n-Hexane Diffusion in Silicalite. Proc. R. Soc. Lond. A. 448, 143–160.
16. Hussain, I., Titiloye, J., 2005. Molecular Dynamics Simulations of the Adsorption and Diffusion Behavior of Pure and Mixed Alkanes in Silicalite. Microporous Mesoporous Mater. 85, 143–156.
17. Jaimes, L., Badillo, M., de Lasa, H.I., 2011. FCC asoline desulfurization using a ZSM-5 Catalyst Interactive Effects of Sulfur Containing Species and Gasoline Components. Fuel 90, 2016–2025.
18. Jaimes, L., Ferreira, M.L., de Lasa, H.I., 2009. Thiophene Conversion under Mild Conditions over a ZSM-5 Catalyst. Chem. Eng. Sci. 64, 2539–2561.
19. Jia, W., Murad, S., 2005. Separation of Gas Mixtures using a Range of Zeolite Membranes: A Molecular Dynamics Study. J. Chem. Phys. 122, 1–11.
20. Jianfen, F., de Graaf, B., Xiao, H.M., Njo, S.L., 1999. Molecular Dynamics Simulation of Ethene Diffusion in MFI and H[Al]ZSM-5. J. Mol. Struct. 492, 133–142.
21. Jobic, H., 2000. Diffusion of Linear and Branched Alkanes in ZSM-5. A Quasi-Elastic Neutron Scattering Study. J. Mol. Catal. A: Chem. 158, 135–142.
22. Jobic, H., Schmidt, W., Krause, C.B., Kärger, J., 2006. PFG NMR and QENS Diffusion Study of n-Alkane Homologues in MFI-Type Zeolites. Microporous Mesoporous Mater. 90, 299–306.
23. Jobic, H., Theodorou, D.N., 2006. Diffusion of Long n-Alkanes in Silicalite. A Comparison between Neutron Scattering Experiments and Hierarchical Simulation Results. J. Phys. Chem. B 110, 1964–1967.
24. Jobic, H., Theodorou, D.N., 2007. Quasi-Elastic Neutron Scattering and Molecular Dynamics Simulation as Complementary Techniques for Studying Diffusion in Zeolites. Microporous Mesoporous Mater. 102, 21–50.
25. June, R.L., Bell, A.T., Theodorou, D.N., 1992. Molecular Dynamics Studies of Butane and Hexane in Silicalite. J. Phys. Chem. 96, 1051–1060.
26. Kärger, J., Pfeifer, H., 1987. NMR elf-Diffusion Studies in Zeolite Science and Technology. Zeolites 7, 90–107.
27. Leroy, F., Rousseau, B., Fuchs, A.H., 2004. Self-Diffusion of n-Alkanes in Silicalite using Molecular Dynamics Simulation: A Comparison between Rigid and Flexible Frameworks. Phys. Chem. Chem. Phys. 6, 775–783.
28. Lins, J.O., Nascimento, M.A., 1997. Molecular Dynamics Studies of Light Hydrocarbon Diffusion in Zeolites. Mol. Eng. 7, 309–316.
29. Liu, Z., Ottaviani, M.F., Abrams, L., Lei, X., Turro, N.J., 2004. Characterization of the External Surface of Silicalites Employing Electron Paramagnetic Resonance. J. Phys. Chem. A 108, 8040–8047.
30. Marcilly, C., 2001. Evolution of Refining and Petrochemicals: What is the Place of Zeolites. Oil Gas Sci. Technol.-Rev. IFP 56, 499–514.
31. McQuaid, M.J., Sun, H., Rigby, D., 2004. Development and Validation of COMPASS Force Field Parameters for Molecules with Aliphatic Azide Chains. J. Comput. Chem. 25, 61–71.
32. Nicholas, J.B., Trouw, F.R., Mertz, J.E., Iton, L.E., Hopfinger, A.J., 1993. Molecular Dynamics Simulation of Propane and Methane in Silicalite. J. Phys. Chem. 97, 4149–4163.
33. Nose, S., 1984. A Unified Formulation of the Constant Temperature Molecular-Dynamics Methods. J. Chem. Phys. 81, 511–519. doi:10.1063/1.447334
34. Ravella, A., de Lasa, H.I., Mahay, A., 1987. Operation and Testing of a Novel Catalytic Reactor Configuration for the Conversion of Methanol to Hydrocarbons. Ind. Eng. Chem. Res. 26, 2546–2552.
35. Roque-Malherbe, R., Wendelbo, R., Mifsud, A., Corma, A., 1995. Diffusion of Aromatic Hydrocarbons in H-ZSM-5, H-Beta, and H-MCM-22 Zeolites. J. Phys. Chem. 99, 14064–14071.
36. Rozanska, X., Van Santen, R.A., 2003. Reaction Mechanisms in Zeolite Catalysis. in: Auerbach, S.M., Carrado, K.A., Dutta, P.K. (Eds.), Handbook of Zeolite Science and Technology, Marcel Dekker Inc., New York. Chapter 15, 900–947.

37. Rungsirisakun, R., Nanok, T., Probst, M., Limtrakul, J., 2006. Adsorption and Diffusion of Benzene in the Nanoporous Catalysts FAU, ZSM-5 and MCM-22: A Molecular Dynamics Study. J. Mol. Graphics Modell. 24, 373–82.
38. Runnebaum, R.C., Maginn, E.J., 1997. Molecular Dynamics Simulations of Alkanes in the Zeolite Silicalite: Evidence for Resonant Diffusion Effects. J. Phys. Chem. B 101, 6394–6408.
39. Samoletov, A.A., Dettmann, C.P., Chaplain, M.A.J., 2007. Thermostats for Slow Configurational Modes. J. Stat. Phys. 128, 1321–1336.
40. Sastre, G., Raj, N., Catlow, C.R.A., Roque-Malherbe, R., Corma, A., 1998. Selective Diffusion of C8 Aromatics in a 10 and 12 MR Zeolite. A Molecular Dynamics Study. J. Phys. Chem. B 102, 3198–3209.
41. Satterfield, C.N., 1980. Heterogeneous Catalysis in Practice, McGraw-Hill Book Company, New York.
42. Schuring, D., 2002. Diffusion in Zeolites: Towards a Microscopic Understanding. PhD Thesis, Eindhoven University of Technology.
43. Smit, B., Daniël J.C. Loyens, L., Verbist, G.L.M.M., 1997. Simulation of Adsorption and Diffusion of Hydrocarbons in Zeolites. Faraday Discuss. 106, 93–104.
44. Song, L., Sun, Z., Rees, L.V.C., 2002. Experimental and Molecular Simulation Studies of Adsorption and Diffusion of Cyclic Hydrocarbons in Silicalite-1. Microporous Mesoporous Mater. 55, 31–49.
45. Sun, H., Ren, P., Fried, J.R., 1998. The COMPASS Forcefield: Parameterization and Validation for Polyphosphazenes. Comput. Theor. Polym. Sci. 8, 229–246.
46. Szczygieł, J., Szyja, B., 2005. Computer Simulated Diffusion of C7 Hydrocarbons in Microporous Materials: Molecular Modeling. Microporous Mesoporous Mater. 83, 85–93.
47. Tukur, N., Al-Khattaf, S., 2005. Catalytic Cracking of n-Dodecane and Alkyl Benzenes over FCC Zeolite Catalysts: Time on Stream and Reactant Converted Models. Chem. Eng. Process. 44, 1257–1268.
48. Verlet, L., 1967. Computer Experiments on Classical Fluids. I. Thermodynamical Properties of Lennard-Jones Molecules. Phys. Rev. 159, 98–103.
49. Xiao, J., 1990. The Diffusion Mechanism of Hydrocarbons in Zeolites. PhD Thesis, Massachusetts Institute of Technology.
50. Xiao, J., Wei, J., 1992a. Diffusion Mechanism of Hydrocarbons in Zeolite I. Theory. Chem. Eng. Sci. 47, 1123–1141.
51. Xiao, J., Wei, J., 1992b. Diffusion Mechanism of Hydrocarbons in Zeolites—II. Analysis of Experimental Observations. Chem. Eng. Sci. 47, 1143–1159.
52. Yu, S., Waku, T., Iglesia, E., 2003. Catalytic Desulfurization of Thiophene on H-ZSM5 Using Alkanes as Co-Reactants. Appl. Catal. A: Gen. 242, 111–121.
53. Zheng, S., 2002. Surface Modification of HZSM-5 Zeolites. PhD Thesis, Technische Universitat München.

Appendix I. Thiophene Adsorption on ZSM5 Zeolite

(a) During the unsteady reaction of benzothiophene in the CREC Riser Simulator, the benzothiophene conversion has to comply with species balances in the ZSM5 crystallite as follows:

$$\frac{\varepsilon D_s}{r^2}\frac{\partial}{\partial r}\left[r^2\frac{\partial C_{bt}}{\partial r}\right]=\frac{\partial C_{bt}}{\partial t}+S_c\rho_c k_{ads}C_{bt}(1-\theta_{bt}-\theta_d)-k_{des}\theta_{bt} \tag{4}$$

and

$$S_c\rho_c k_{ads}C_{bt}(1-\theta_{bt}-\theta_d)-k_{des}\theta_{bt}=\rho_c K_{bt}\frac{\partial C_{bt}}{\partial t}+\text{Catalytic Reaction Rate} \tag{5}$$

With εD_s in m^2/s representing the effective diffusivity, k_{ads} the intrinsic rate adsorption constant in m/s, k_{des} the intrinsic rate desorption constant in moles/ (m^2 s), C_{bt} the benzothiophene concentration in mole/m^3, K_{bt} the benzothiophene equilibrium adsorption constant in m^3/g, S_c the specific crystallite area per unit weight in m^2/g, ρ_c the apparent crystallite density in g/m^3 and θ_{bt} and θ_d the dimensionless site fraction occupied by benzothiophene and n-dodecane.

As a result, one can notice that both benzothiophene and the n-dodecane occupied sites influence the adsorption processes.

(b) However, during the early stages of adsorption, one can postulate a simplified (eq. (1)) with: i) no sites occupied by dodecane species, $\theta_d = 0$, ii) very small fractions of sites being occupied by benzothiophene $\theta_{bt} \ll 1$, and iii) catalytic reaction being negligible.

Thus,

$$\frac{\epsilon D_s}{r^2}\frac{\partial}{\partial r}\left[r^2\frac{\partial C_{bt}}{\partial r}\right]=\varepsilon\frac{\partial C_{bt}}{\partial t}+S_c\rho_c k_{ads}C_{bt} \tag{6}$$

and

$$S_c\rho_c[k_{ads}C_{bt}]=\rho_c K_{bt}\frac{\partial C_{bt}}{\partial t} \tag{7}$$

One should notice that under these early unsteady conditions a large $\frac{\varepsilon D_s}{r^2}\frac{\partial}{\partial r}\left[r^2\frac{\partial C_{bt}}{\partial r}\right]$ leads to significant selective benzothiophene adsorption with no n-dodecane occupied sites.